

# SOME MORE ON LOGARITHMIC SINGULARITY INTEGRATION IN BOUNDARY ELEMENT METHOD

Tomasz Rymarczyk<sup>1,2</sup>, Jan Sikora<sup>1,2</sup>

<sup>1</sup>Research & Development Centre Netrix S.A., Lublin, Poland, <sup>2</sup>University of Economics and Innovation in Lublin, Faculty of Transport and Informatics, Lublin, Poland

**Abstract.** The accuracy of calculations of integrals with logarithmic singularities for two methods, namely the method of ignoring singularities and the method of subtraction (consisting in separating the singular part from the remaining non-singular), are presented in this paper. Only two-dimensional problems, like Dirichlet's problems, as well as acoustic problems formulated in the frequency domain are considered. Problems related to the accuracy of calculations are discussed and the influence of frequency, as well as the influence of the geometry of the analysed area on the accuracy of calculations, are indicated. When we talk about the influence of geometry, we mean not only discretization, but also the configuration of the area, such as the sharp edges of the boundary line, assuming the use of the classic, without any modifications, Boundary Element Method.

**Keywords:** singular integral calculating, ignoring singularity method, singularity subtraction technique, acoustic wave propagation, Boundary Element Method (BEM)

## JESZCZE O CAŁKOWANIU LOGARYTMICZNYCH OSOBLIWOŚCI W METODZIE ELEMENTÓW BRZEGOWYCH

**Streszczenie.** Dokładność obliczeń całek z osobliwościami logarytmicznymi dla dwóch metod a mianowicie metody ignorowania osobliwości i metody odjęcia (polegającej na wyodrębnieniu części osobliwej od pozostałej nieosobliwej), zostały przedstawione w tym artykule. Rozważono jedynie zagadnienia dwuwymiarowe zagadnienia Dirichleta jak również zagadnienia akustyczne sformułowane w dziedzinie częstotliwości. Omówiono problemy związane z dokładnością obliczeń oraz wskazano na wpływ częstotliwości a także wpływ geometrii analizowanego obszaru na dokładność obliczeń. Mówiąc o wpływie geometrii mamy na myśli nie tylko dyskretyzację, ale także konfigurację rozpatrywanego obszaru jak na przykład ostre krawędzie linii brzegowej przy założeniu stosowania klasycznej, bez żadnych modyfikacji, Metody Elementów Brzegowych.

**Słowa kluczowe:** liczenie całek osobliwych, metoda ignorowania osobliwości, metoda izolacji osobliwości, propagacja fal akustycznych, Metoda Elementów Brzegowych (MEB)

### Introduction

The singular integration is a genuine problem for the Boundary Element Method, and it has a considerable influence on the final precision of calculation. The more complicated problem the more sensitive on the singularity Boundary Element Method (BEM) software is.

For the acoustic problems, the extensive review of singular integration is provided by S.M. Kirkup et al in an excellent work [3]. The authors presented several methods like:

1. ignoring the singularity,
2. subtracting out the singularity, (singularity subtraction technique)
3. product integration,
4. substitution or transformation.

In this paper only first two of those method would be considered for two dimensional problems.

### 1. Fundamental equations and discretization by second order boundary elements

The second order boundary elements have some well-known advantages and disadvantages as well [1, 3–5]. In the subsequent sections we would like to look closely in the problem of singular integrals calculation.

The first of the methods mentioned above seems to be the simplest one. In case of quadratic boundary elements, the numerical integration of the kernels could be done in a similar way as for constant and linear elements. The Jacobian of transformation and the components of unit outward normal vector are calculated according to the following equations:

$$J(\xi) = \frac{d\Gamma}{d\xi} = \sqrt{\left(\frac{dx(\xi)}{d\xi}\right)^2 + \left(\frac{dy(\xi)}{d\xi}\right)^2} \quad (1)$$

The components of unit outward normal are functions of local coordinate  $\xi$ :

$$n_x(\xi) = \frac{1}{J(\xi)} \left[ \frac{dy(\xi)}{d\xi} \right], \quad n_y(\xi) = -\frac{1}{J(\xi)} \left[ \frac{dx(\xi)}{d\xi} \right] \quad (2)$$

It is important to notice that the choice of local coordinate system from -1 to +1 was not arbitrary, because it happens to be the same as limits used in Gaussian quadrature technique [2].

The boundary curve  $\Gamma$  is now divided into elements  $\Gamma_j$  and the numerical integration performed over each element using the local intrinsic coordinate  $\xi$  rather than the boundary segment  $\Gamma_j$ .

$$\int_{\Gamma_j} f(x, y) d\Gamma = \int_{-1}^{+1} f(x(\xi), y(\xi)) J(\xi) d\xi \quad (3)$$

where  $f$  means any function.

Let's carry out numerical experiment using the Dirichlet problem in the homogeneous region shown in Fig. 1.

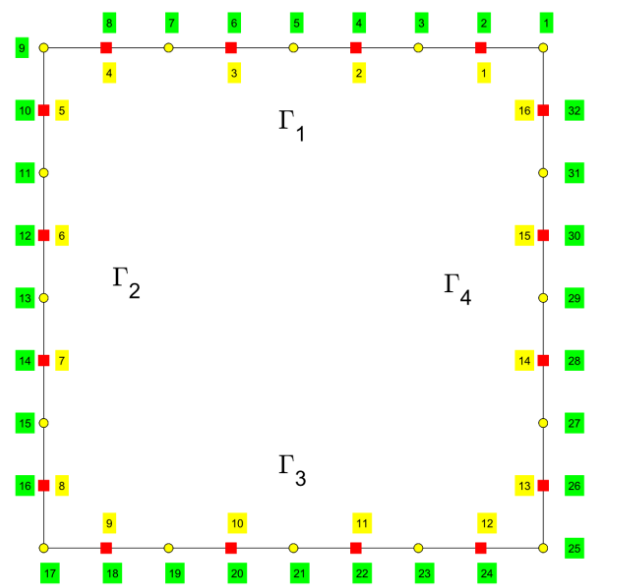


Fig. 1. Example of discretization of the homogeneous region by second order boundary elements with nodes numbering (counterclockwise direction on the green background) and elements numbering (inside subregion with yellow background)

The region consists of the square area bounded by four lines denoted as  $\Gamma$  (see Fig. 1). In the upper  $\Gamma_1$  and lower part  $\Gamma_3$  of the boundary Dirichlet boundary conditions are imposed but on a vertical parts  $\Gamma_2$  and  $\Gamma_4$  Neumann homogeneous boundary conditions are defined.



Let us consider Dirichlet Problem presented in Fig. 1. The boundary of the region under consideration will be divided into  $M$  quadratic boundary elements as it is shown in Fig. 3. The nodes with the unknown values, in all three nodes of each boundary element are considered. Let consider the following integral equation [5, 7] describing distribution of electric potential inside of the region (see Fig. 1):

$$c(\mathbf{r})\varphi(\mathbf{r}) + \int_{\Gamma} \frac{\partial G(|\mathbf{r} - \mathbf{r}'|)}{\partial n} \varphi(\mathbf{r}') d\Gamma(\mathbf{r}') = \int_{\Gamma} G(|\mathbf{r} - \mathbf{r}'|) \frac{\partial \varphi(\mathbf{r}')}{\partial n} d\Gamma(\mathbf{r}') \quad (4)$$

$$\text{where } c(\mathbf{r}) = \begin{cases} 1 & \text{for the external problems} \\ +0.5 & \text{for the smooth boundary line} \\ 1 - \frac{\gamma}{2\pi} & \text{angle } \gamma \text{ is shown in the Fig. 2} \end{cases}$$

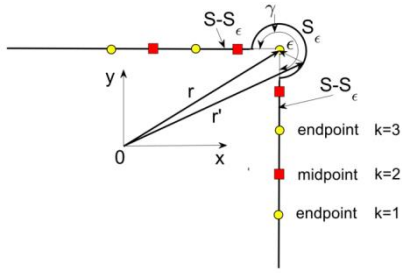


Fig. 2. Boundary point  $\mathbf{r}$  is in the corner

The numerical integration is performed over each boundary element  $\Gamma_j$  using the local intrinsic coordinate  $\xi$ , as follows:

$$c(\mathbf{r})\varphi_i(\mathbf{r}) + \sum_{j=1}^M \int_{-1}^{+1} \sum_{k=1}^3 \frac{\partial G(|\mathbf{r} - \mathbf{r}'|)}{\partial n} N_k(\xi) (\varphi_k(\mathbf{r}'))_j J(\xi) d\xi = \sum_{j=1}^M \int_{-1}^{+1} \sum_{k=1}^3 G(|\mathbf{r} - \mathbf{r}'|) N_k(\xi) (q_k(\mathbf{r}'))_j J(\xi) d\xi \quad (5)$$

where  $M$  – is the total number of quadratic elements and for simplicity lets denote the normal derivative by  $\left(\frac{\partial \varphi_k(\mathbf{r}')}{\partial n}\right)_j = (q_k(\mathbf{r}'))_j$  (see Fig. 4).

We can define a new coordinate system that is local to the element using an intrinsic variable  $\xi$  (Eq. 7–9), with its origin at the midpoint of the element and values of -1 and +1 at the end nodes as it is shown in Fig. 3.

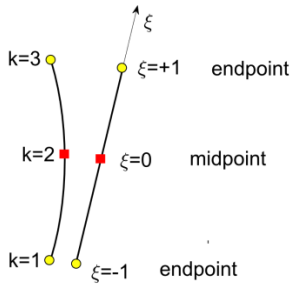


Fig. 3. Transformation from cartesian to the local coordinate system for the isoparametric quadratic element

$$\mathbf{r} = (x(\xi), y(\xi)) \quad (6)$$

where  $\mathbf{r}$  is the position vector of the nodes.

$$x(\xi) = \sum_{k=1}^3 N_k(\xi) x_k = N_1(\xi)x_1 + N_2(\xi)x_2 + N_3(\xi)x_3 \quad (7)$$

$$y(\xi) = \sum_{k=1}^3 N_k(\xi) y_k = N_1(\xi)y_1 + N_2(\xi)y_2 + N_3(\xi)y_3 \quad (8)$$

where  $N_k(\xi)$  are quadratic functions such as:  $N_k(\xi) = 1$  at its own node for example the node  $k = 1$  and  $N_k(\xi) = 0$  at the other two nodes  $k = 2$  and  $k = 3$ , resulting in the following:

$$\begin{aligned} N_1(\xi) &= -\frac{\xi}{2}(1 - \xi) = 0.5\xi(1 - \xi) \\ N_2(\xi) &= (1 + \xi)(1 - \xi) = 1 - \xi^2 \\ N_3(\xi) &= +\frac{\xi}{2}(1 + \xi) = 0.5\xi(1 + \xi) \end{aligned} \quad (9)$$

Using the isoparametric elements the same basis functions are used for interpolation both variables  $\varphi(\xi)$  and  $q = \frac{\partial \varphi(\xi)}{\partial n}$ :

$$\varphi(\xi) = \sum_{k=1}^3 N_k(\xi) \varphi_k = N_1(\xi)\varphi_1 + N_2(\xi)\varphi_2 + N_3(\xi)\varphi_3 \quad (10)$$

and

$$\begin{aligned} \frac{\partial \varphi(\xi)}{\partial n} &= \sum_{k=1}^3 N_k(\xi) \frac{\partial \varphi_k}{\partial n} = \\ &= N_1(\xi) \frac{\partial \varphi_1}{\partial n} + N_2(\xi) \frac{\partial \varphi_2}{\partial n} + N_3(\xi) \frac{\partial \varphi_3}{\partial n} \end{aligned} \quad (11)$$

The Jacobian of transformation and components of unit outward normal vector are calculated according to Eq. (1) and Eq. (2) respectively.

The second term in Eq. (2) for  $n_x(\xi)$  and for  $n_y(\xi)$  could be expressed in a following way:

$$\frac{dx(\xi)}{d\xi} = \frac{dN_1(\xi)}{d\xi} x_1 + \frac{dN_2(\xi)}{d\xi} x_2 + \frac{dN_3(\xi)}{d\xi} x_3 \quad (12)$$

$$\frac{dy(\xi)}{d\xi} = \frac{dN_1(\xi)}{d\xi} y_1 + \frac{dN_2(\xi)}{d\xi} y_2 + \frac{dN_3(\xi)}{d\xi} y_3 \quad (13)$$

and differentials of the shape functions are easily determined basing on Eq. (9):

$$\begin{aligned} \frac{dN_1(\xi)}{d\xi} &= \frac{d}{d\xi} \left( -\frac{\xi}{2}(1 - \xi) \right) = \xi - \frac{1}{2} \\ \frac{dN_2(\xi)}{d\xi} &= \frac{d}{d\xi} \left( (1 + \xi)(1 - \xi) \right) = -2\xi \\ \frac{dN_3(\xi)}{d\xi} &= \frac{d}{d\xi} \left( +\frac{\xi}{2}(1 + \xi) \right) = \xi + \frac{1}{2} \end{aligned} \quad (14)$$

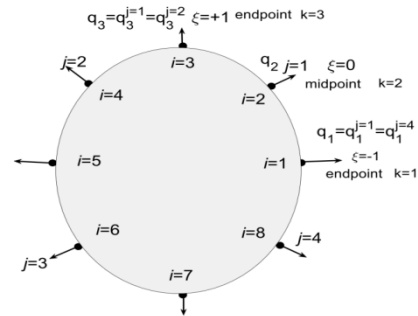


Fig. 4. Smooth boundary discretization for the quadratic boundary elements

The numerical integration is performed over each boundary element  $\Gamma_j$  using the local coordinate  $\xi$  (see Fig. 3). The nodal values are constant, so we can finally rewrite Eq. (5) in the following form:

$$\begin{aligned} c(\mathbf{r})\varphi_i(\mathbf{r}) + \sum_{j=1}^M \sum_{k=1}^3 (\varphi_k(\mathbf{r}'))_j \int_{-1}^{+1} N_k(\xi) \frac{\partial G(|\mathbf{r} - \mathbf{r}'|)}{\partial n} d\xi = \\ = \sum_{j=1}^M \sum_{k=1}^3 (q_k(\mathbf{r}'))_j \int_{-1}^{+1} N_k(\xi) G(|\mathbf{r} - \mathbf{r}'|) d\xi \end{aligned} \quad (15)$$

If we denote the terms containing the integrals of the kernel's normal derivative  $\frac{\partial G(|\mathbf{r} - \mathbf{r}'|)}{\partial n}$  and  $G(|\mathbf{r} - \mathbf{r}'|)$  as  $a_{j,k}^{(j)}$  and  $b_{j,k}^{(j)}$  respectively, we will get:

$$a_{i,k}^{(j)}(\mathbf{r}, \mathbf{r}') = \int_{-1}^{+1} N_k(\xi) \frac{\partial G(|\mathbf{r} - \mathbf{r}'|)}{\partial n} J_j(\xi) d\xi \quad (16)$$

$$b_{i,k}^{(j)}(\mathbf{r}, \mathbf{r}') = \int_{-1}^{+1} N_k(\xi) G(|\mathbf{r} - \mathbf{r}'|) J_j(\xi) d\xi \quad (17)$$

For the smooth boundary, the integral functions  $a_{j,k}^{(j)}$  and  $b_{j,k}^{(j)}$  can be lumped together in the global functions  $A_{i,j}$  and  $B_{i,j}$  as follows:

$$\begin{aligned} c(\mathbf{r})\varphi_i(\mathbf{r}) + \sum_{j=1}^M \sum_{k=1}^3 (\varphi_k(\mathbf{r}'))_j a_{i,k}^{(j)}(\mathbf{r}, \mathbf{r}') = \\ = \sum_{j=1}^M \sum_{k=1}^3 (q_k(\mathbf{r}'))_j b_{i,k}^{(j)}(\mathbf{r}, \mathbf{r}') \end{aligned} \quad (18)$$

and:

$$\begin{aligned} c(\mathbf{r})\varphi_i(\mathbf{r}) + \sum_{j=1}^M \varphi_j(\mathbf{r}) A_{i,j}(\mathbf{r}, \mathbf{r}') = \\ = \sum_{j=1}^M q_j(\mathbf{r}) B_{i,j}(\mathbf{r}, \mathbf{r}') \end{aligned} \quad (19)$$

where  $\mathbf{r}$  depends on index  $i$  and  $\mathbf{r}'$  depends on index  $j$  (see Fig. 4).

## 2. Numerical integration of the Kernel

To form a set of linear algebraic equations, we take each node in turn as a load point  $\mathbf{r}$  and perform the integrations indicated in Eq. (16) and in Eq. (17) as well as in Eq. (19):

$$[\mathbf{A}][\boldsymbol{\varphi}] = [\mathbf{B}] \left[ \frac{\partial \boldsymbol{\varphi}}{\partial n} \right] \quad (20)$$

where the matrices  $[\mathbf{A}]$  and  $[\mathbf{B}]$  contain the integrals of the kernel's normal derivative  $\frac{\partial G(|\mathbf{r}-\mathbf{r}'|)}{\partial n}$  and the kernels  $G(|\mathbf{r}-\mathbf{r}'|)$  respectively, i.e., the functions  $A_{i,j}$  and  $B_{i,j}$  of Eq. (19).

If  $R$  denotes the distance between point  $\mathbf{r}$  and point  $\mathbf{r}'$  then:

$$R = |\mathbf{r} - \mathbf{r}'| = \sqrt{(x - x')^2 + (y - y')^2} \quad (21)$$

The normal derivative of Green's function in case of Laplace equation is:

$$\begin{aligned} \frac{\partial G(|\mathbf{r}-\mathbf{r}'|)}{\partial n} &= \frac{\partial G}{\partial R} \frac{\partial R}{\partial n} = \frac{\partial G}{\partial R} \left[ \frac{\partial R}{\partial x'} \frac{\partial x'}{\partial n} + \frac{\partial R}{\partial y'} \frac{\partial y'}{\partial n} \right] = \\ &= -\frac{1}{2\pi R^2} [(x' - x)n_{x'} + (y' - y)n_{y'}] \end{aligned} \quad (22)$$

where:

$$\frac{\partial R}{\partial x'} = \frac{x' - x}{R}; \quad \frac{\partial R}{\partial y'} = \frac{y' - y}{R} \quad (23)$$

$$\frac{\partial x'}{\partial n} = n_{x'}; \quad \frac{\partial y'}{\partial n} = n_{y'} \quad (24)$$

where  $n_{x'}$  and  $n_{y'}$  are defined by Eq. (1) and Eq. (2) under one condition that  $x$  must be replaced by  $x'$  and the same for  $y$  coordinate.

In case of non-singular integrals, point  $\mathbf{r}'$  never meet point  $\mathbf{r}$  the standard Gauss-Legendre quadrature can be easily applicable to integrals of the general form:

$$\int_{-1}^{+1} f(\xi) d\xi = \sum_{i=1}^{ng} w_i f(\xi_i), \quad (25)$$

where  $ng$  is the total number of Gaussian integration points, and  $\xi_i$  is the Gaussian coordinate with an associated weight function  $w_i$ . The most frequently used values are listed in the literature under the following address [9].

## 3. Ignoring the singularity

When the kernels are the regular functions, it is quite easy to integrate them according to Eq. (25). But when the point  $\mathbf{r}$  lay in the same boundary element as point  $\mathbf{r}'$  the singularity will become a problem. There are some special methods to deal with them which was mentioned in the introduction.

All methods mentioned in the introduction are very interesting but let us start with the first one, which seems to be the simplest one.

As a test of the proposed approach, let us consider the area of the unit square with mixed Dirichlet-Neumann boundary conditions (Fig. 1). On the edges parallel to the  $x$ -axis, on the upper part of edge the potential  $\varphi = 10$  and on the lower part of edge  $\varphi = -10$ . On the vertical edges relative to the  $x$ -axis, homogeneous Neumann boundary conditions were imposed. Physically, this corresponds to a flat capacitor but without edge effects. The square area is trivial, but due to the selected boundary element of the second order and the non-smooth shape of the boundary, the task is not trivial at all, particularly if we use the classical boundary element method (Fig. 2). The analytical solution is known, so there is a possibility to calculate errors. The first approach, named as ignoring singularities, is conceptually the simplest one, but as it turns out, it leads to an excessive number of integration points in numerical Gauss quadrature, providing barely satisfactory accuracy of calculations (see Fig. 5).

This approach to singular integrals, unfortunately, as we see in Fig. 5, leads to a vast number of Gaussian integration points. Therefore, this method, which is undoubtedly characterized by simplicity, but at the expense of excessive numerical operations, should be considered as not interesting.

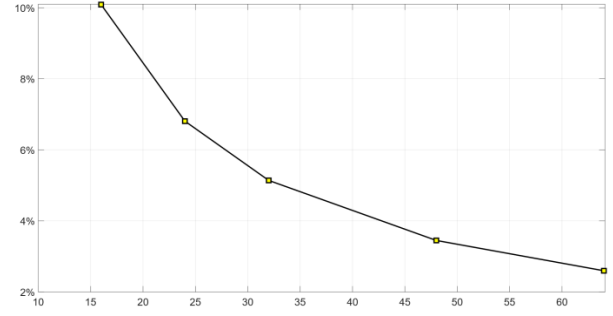


Fig. 5. Accuracy versus number of Gaussian integration points of BEM calculation of the test problem

## 4. Subtracting out the singularity approach

The case of weakly singular integration occurs when the collocation node lies inside the integration element and if the singularity is of the order  $O(\ln(1/R))$  for two-dimensional problem. One of the methods dealing with such singularity is the subtraction method [3]. Integrand first must be separated into singular and non-singular parts. In case of quadratic boundary elements, the numerical integration of the kernels could be done in an analogous way as for constant element [5, 6]. The Jacobian of transformation and the components of unit outward normal are calculated according to Eq. (1) and Eq. (2).

The first derivative of the original coordinates for the second order element are expressed by Eq. (7) and Eq. (8) also by Eq. (12) and Eq. (13).

Dealing first with the second kernel  $G(|\mathbf{r}-\mathbf{r}'|)$  (see Eq. 15) we have to consider two cases. The first case when load and field points are in different elements. Then integrals are not singular. And a bit more difficult problem when those two points are in the same element. In this case the singularity may occur in all three nodes of the quadratic boundary element. Then to calculate the integrals we must consider the following three cases:

1. the point  $\mathbf{r}$  is the first node ( $k = 1$ ) of the element,
2. the point  $\mathbf{r}$  is the second node ( $k = 2$ ) of the element,
3. the point  $\mathbf{r}$  is the third node ( $k = 3$ ) of the element.

The distance between point  $\mathbf{r}$  and point  $\mathbf{r}'$  was denoted by  $R$  (see Eq. 21). So, for the first node:

$$\begin{aligned} R^2 &= (x_1 - x'(\xi))^2 + (y_1 - y'(\xi))^2 = \\ &= [N_1(\xi)x_1 + N_2(\xi)x_2 + N_3(\xi)x_3 - x_1]^2 + \\ &\quad + [N_1(\xi)y_1 + N_2(\xi)y_2 + N_3(\xi)y_3 - y_1]^2 \end{aligned} \quad (26)$$

where  $N_1(\xi)$ ,  $N_2(\xi)$  and  $N_3(\xi)$  are expressed by Eq. (9).

So:

$$\begin{aligned} R^2 &= \\ &= \left[ -\frac{\xi}{2}(1-\xi)x_1 + (1-\xi)(1+\xi)x_2 + \frac{\xi}{2}(1+\xi)x_3 - x_1 \right]^2 + \\ &\quad + \left[ -\frac{\xi}{2}(1-\xi)y_1 + (1-\xi)(1+\xi)y_2 + \frac{\xi}{2}(1+\xi)y_3 - y_1 \right]^2 \end{aligned} \quad (27)$$

In an analogous way, we can write the distance  $R$  for the next nodes, the second one:

$$\begin{aligned} R^2 &= \\ &= \left[ -\frac{\xi}{2}(1-\xi)x_1 + (1-\xi)(1+\xi)x_2 + \frac{\xi}{2}(1+\xi)x_3 - x_2 \right]^2 + \\ &\quad + \left[ -\frac{\xi}{2}(1-\xi)y_1 + (1-\xi)(1+\xi)y_2 + \frac{\xi}{2}(1+\xi)y_3 - y_2 \right]^2 \end{aligned} \quad (28)$$

and the third one:

$$\begin{aligned} R^2 &= \\ &= \left[ -\frac{\xi}{2}(1-\xi)x_1 + (1-\xi)(1+\xi)x_2 + \frac{\xi}{2}(1+\xi)x_3 - x_3 \right]^2 + \\ &\quad + \left[ -\frac{\xi}{2}(1-\xi)y_1 + (1-\xi)(1+\xi)y_2 + \frac{\xi}{2}(1+\xi)y_3 - y_3 \right]^2 \end{aligned} \quad (29)$$

Equations (27-29) shows how the distant  $R$  could be calculated. However, when the points  $\mathbf{r}$  and  $\mathbf{r}'$  are in the same element but  $\mathbf{r} \neq \mathbf{r}'$  the kernels are singular but the shape function  $N_k(\xi)$  in the vicinity of  $\mathbf{r}$  is of the order  $r$ . Therefore, the product of the kernels and the shape function is not singular, and the integrals can be evaluated using the standard Gaussian quadrature (see Eq. (25)). So far, all the off-diagonal coefficients of the matrices  $[\mathbf{A}]$  and  $[\mathbf{B}]$  (see Eq. (20)) have been calculated.

In case, when the points  $\mathbf{r}$  and  $\mathbf{r}'$  are in the same element but  $\mathbf{r} \rightarrow \mathbf{r}'$ , so distance  $R \rightarrow 0$  the standard Gaussian quadrature cannot be used, because of the singularity of the kernels. Dealing with the kernel  $G_0(\mathbf{r}, \mathbf{r}') = \frac{1}{2\pi} \ln \frac{1}{R}$ , it is clear that as  $\mathbf{r}$  coincides with  $\mathbf{r}'$ , the singularity is of the form  $\ln(1/\eta)$  as  $\eta \rightarrow 0$ . Fortunately, this form of integral can be calculated by using the special logarithmic Gaussian quadrature scheme given below:

$$\int_0^1 f(\eta) \ln \frac{1}{\eta} d\eta = \sum_{i=1}^{gl} w_i f(\eta_i) \quad (30)$$

where  $gl$  is the total number of logarithmic Gaussian integration points used and  $\eta_i$  is the Gaussian coordinate with an associated weight function  $w_i$  [5]. Note that the limits of integration are now from 0 to 1 instead of the  $-1$  to  $+1$  range used in the non-singular integrals.

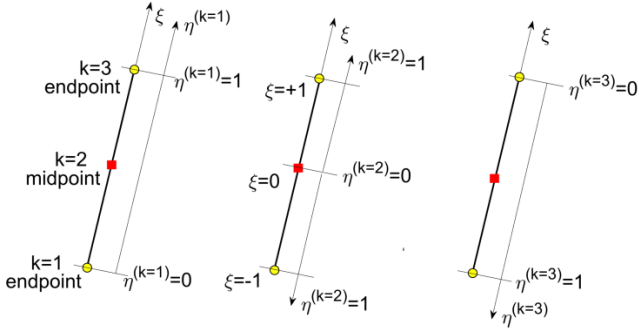


Fig. 6. Coordinates transformation. a)  $\mathbf{r}$  is in the first node of the element, b) second node and c) third node

A simple linear transformation can be used to transform the integral variable from  $\xi$  to  $\eta$  (see Fig. 6) as follows:

1. if the position vector  $\mathbf{r}$  is the first node ( $k = 1$ ) of the element:  $\eta^{(k=1)} = 0.5(1 + \xi)$ ,

2. if the position vector  $\mathbf{r}$  is the second node ( $k = 2$ ) of the element – the element is divided into two sub – elements (see Fig. 6b):

for  $-1 < \xi < 0$   $\eta^{(k=2)} = -\xi$  and for  $0 < \xi < +1$   $\eta^{(k=2)} = \xi$ ,

3. if the position vector  $\mathbf{r}$  is the third node ( $k = 3$ ) of the element:  $\eta^{(k=3)} = 0.5(1 - \xi)$ .

For the first node the Eq. (27) can be rearranged in the following way:

$$\begin{aligned} R^2 &= [0.5(1 + \xi)]^2 \cdot \\ &\cdot \{[(\xi - 2)x_1 + 2(1 - \xi)x_2 + \xi x_3]^2 + \\ &+ [(\xi - 2)y_1 + 2(1 - \xi)y_2 + \xi y_3]^2\} = \\ &= (\eta^{(1)})^2 \left[ \left( f_x^{(1)}(\xi) \right)^2 + \left( f_y^{(1)}(\xi) \right)^2 \right] \end{aligned} \quad (31)$$

For the second node the Eq. (28) can be rearranged in the following way:

$$\begin{aligned} R^2 &= \\ &= \xi^2 \{ [0.5(\xi - 1)x_1 - \xi x_2 + 0.5(\xi + 1)x_3]^2 + \\ &+ [0.5(\xi - 1)y_1 - \xi y_2 + 0.5(\xi + 1)y_3]^2 \} = \\ &= (\eta^{(2)})^2 \left[ \left( f_x^{(2)}(\xi) \right)^2 + \left( f_y^{(2)}(\xi) \right)^2 \right] \end{aligned} \quad (32)$$

For the third node the Eq. (29) can be rearranged in the following way:

$$\begin{aligned} R^2 &= \\ &= [0.5(1 - \xi)]^2 \{ [-\xi x_1 + 2(1 + \xi)x_2 - 2(2 + \xi)x_3]^2 + \\ &+ [-\xi y_1 + 2(1 + \xi)y_2 - 2(2 + \xi)y_3]^2 \} = \\ &= (\eta^{(3)})^2 \left[ \left( f_x^{(3)}(\xi) \right)^2 + \left( f_y^{(3)}(\xi) \right)^2 \right] \end{aligned} \quad (33)$$

Therefore, a general expression can be written for the logarithmic term as follows:

$$\begin{aligned} G_0(|\mathbf{r} - \mathbf{r}'|) &= \frac{1}{2\pi} \ln \frac{1}{|\mathbf{r} - \mathbf{r}'|} = \frac{1}{2\pi} \ln \frac{1}{(\eta^{(k)})^2 \left[ \left( f_x^{(k)}(\xi) \right)^2 + \left( f_y^{(k)}(\xi) \right)^2 \right]} = \\ &= \frac{1}{2\pi} \ln \frac{1}{(\eta^{(k)})^2} - \frac{1}{2\pi} \frac{1}{2} \ln \left[ \left( f_x^{(k)}(\xi) \right)^2 + \left( f_y^{(k)}(\xi) \right)^2 \right] \end{aligned} \quad (34)$$

where:  $k$  indicates, the node number and  $\eta^{(k)}$  transforms the integration limits from  $(-1$  to  $+1)$  to  $(0$  to  $+1)$  and changes integrand value according to the position of  $\mathbf{r}$  in the element.

So, for quadratic boundary element the kernel as  $\mathbf{r}'$  approaches  $\mathbf{r}$ , can be split into two distinct parts: logarithmic part (with singularity) and a non-logarithmic (regular) one (see first and the second term of Eq. (34)). Dealing now with the logarithmic part of the kernel, it can be shown that it contains terms of order  $\frac{1}{\eta}$  as  $\eta \rightarrow 0$ .

Therefore, we can no longer use the Gaussian quadrature technique, even if a large number of Gaussian points are used. Furthermore, we also need to explicitly calculate the parameter  $c(\mathbf{r})$  (see Eq. 4) because its contribution is added to the diagonal terms of the  $[\mathbf{A}]$  matrix. This problem is particularly important in cases where the boundary line is not smooth as it is shown for the example in Fig. 1 and Fig. 2. However, because all non-diagonal coefficients of the  $[\mathbf{A}]$  matrix can be calculated, there is a way to overcome this problem (see Eq. 4) [1].

## 5. Subtracting out the singularity in case of the constant element discretization for acoustic problems

Above the second approach subtracting out singularity was presented for the second order boundary element in case of Laplace's equation. The singular integral is divided into logarithmic (singular) and regular (non-singular) parts. This approach, as shown above, seems to be laborious and can only be directly applied to the Laplace equation.

So, arise a question how we can treat more complicated problems. We will show subtracting out singularity procedure for acoustic problem, however for constant boundary element for simplicity.

This method is widely applied in BEM code and provide high precision solution [1, 3, 8]. In this case integrand would be split onto two parts the singular part and the regular one in the following way. For example, if  $f(x) \sim \psi(x)$  near to the singularity then writing  $f(x) = \psi(x) + [f(x) - \psi(x)]$  the first term  $\psi(x)$  might be singular but the last one  $f(x) - \psi(x)$  may be regular one.

The singularity does not disappear but  $\int \psi(x) dx$  in some cases (for example the Laplace's equation) it could be calculated analytically. This is a general approach and could be used not necessarily in acoustic but in many other problems.

$$\begin{aligned} \int_{\Gamma} G(|\mathbf{r} - \mathbf{r}'|) d\Gamma &= \int_{\Gamma} [G(|\mathbf{r} - \mathbf{r}'|) - G_0(|\mathbf{r} - \mathbf{r}'|)] d\Gamma + \\ &+ \int_{\Gamma} G_0(|\mathbf{r} - \mathbf{r}'|) d\Gamma \end{aligned} \quad (35)$$

For 2D system, the fundamental solution for the Laplace's equation is equal:

$$\begin{aligned} \int_{\Gamma} G_0(|\mathbf{r} - \mathbf{r}'|) d\Gamma &= \frac{1}{2\pi} \ln \frac{1}{|\mathbf{r} - \mathbf{r}'|} = \\ &= -\frac{1}{2\pi} \ln \sqrt{(x - x')^2 + (y - y')^2} = \\ &= -\frac{1}{2\pi} \frac{1}{2} \ln((x - x')^2 + (y - y')^2) \end{aligned} \quad (36)$$

The distance  $R$  (see Eq. (21)) between point  $\mathbf{r}$  and point  $\mathbf{r}'(\xi)$  depends on local coordinate system as Eq. (21) shows. Consequently, the main diagonal term of the  $[\mathbf{B}]$  matrix (Eq. (20)) could be expressed in the following way:

$$b_{i,k}^{(j)}(\mathbf{r}, \mathbf{r}') = \int_{-1}^{+1} N_k(\xi) G_0(|\mathbf{r} - \mathbf{r}'|) J_j(\xi) d\xi \quad (37)$$

To solve more advanced acoustic problems, let us start with the excellent benchmark problem suggested by S. Kirkup in [3].

Let us consider the air as an acoustic environment at 20°C and the pressure is one atmosphere (one atm is equal to 101.325 kPa). The speed of sound is equal to 344 m/s and the frequency of the test is within the range 300 up to 1200 Hz, hence  $k = 5.48 \div 21.92 \text{ m}^{-1}$  and the wavelength  $\lambda = \frac{c}{f} = 1.15 \div 0.29 \text{ m}$ .

The region of the benchmark is like this one presented in Fig. 1, but this time discretized by constant boundary element for simplicity, just to show how the subtracting method works even for more complicated, from physical point of view, examples.

$$\int_{\Gamma} G(|\mathbf{r} - \mathbf{r}'|) d\Gamma = \int_{\Gamma} G_0(|\mathbf{r} - \mathbf{r}'|) d\Gamma + \int_{\Gamma} [G(|\mathbf{r} - \mathbf{r}'|) - G_0(|\mathbf{r} - \mathbf{r}'|)] d\Gamma \quad (38)$$

For 2D problem exists the analytical expression for the integral  $\int_{\Gamma} G_0(|\mathbf{r} - \mathbf{r}'|) d\Gamma$ , then for acoustic problem described by the Helmholtz equation (38) we will get (consult for example [3, 8]):

$$\begin{aligned} G(|\mathbf{r} - \mathbf{r}'|) - G_0(|\mathbf{r} - \mathbf{r}'|) &= \frac{i}{4} H_0^{(1)}(kR) - \frac{-1}{2\pi} \ln(R) = \\ &= \frac{i}{4} (J_0(kR) + iY_0(kR)) + \frac{1}{2\pi} \ln(R) = \\ &= -\frac{1}{4} Y_0(kR) + \frac{1}{2\pi} \ln(R) + \frac{i}{4} J_0(kR) \end{aligned} \quad (39)$$

where:  $J_0$  and  $Y_0$  are the Spherical Bessel functions of the first and the second kind respectively and  $R$  is defined by Eq. (21).

In acoustic problems described in a frequency domain integral formulation is:

$$\begin{aligned} c(\mathbf{r})\varphi(\mathbf{r}) + \int_{\Gamma} \frac{\partial G(|\mathbf{r} - \mathbf{r}'|)}{\partial n} \varphi(\mathbf{r}') d\Gamma = \\ = \int_{\Gamma} G(|\mathbf{r} - \mathbf{r}'|) \frac{\partial \varphi(\mathbf{r}')}{\partial n} d\Gamma \end{aligned} \quad (40)$$

where  $c(\mathbf{r})$  is defined by Eq. (4).

Now the boundary integral equation Eq. (40) for constant boundary elements can be written in terms of local coordinate  $\xi$  instead of the boundary line  $\Gamma$ , as follows:

$$\begin{aligned} c(\mathbf{r})\varphi(\mathbf{r}) + \sum_{j=1}^M \varphi_j(\mathbf{r}') \int_{-1}^{+1} \frac{\partial G(|\mathbf{r} - \mathbf{r}'|)}{\partial n} J(\xi) d\xi = \\ = \sum_{j=1}^M \frac{\partial \varphi_j(\mathbf{r}')}{\partial n} \int_{-1}^{+1} G(|\mathbf{r} - \mathbf{r}'|) J(\xi) d\xi \end{aligned} \quad (41)$$

where  $M$  – is the total number of constant elements, and  $J(\xi)$  – is the Jacobian of transformation (see Eq. (1)).

The functions under integral sign which contain the kernels can be substituted by the functions  $A_{i,j}$  and  $B_{i,j}$  as follows:

$$\begin{aligned} c(\mathbf{r})\varphi(\mathbf{r}) + \sum_{j=1}^M \varphi_j(\mathbf{r}') A_{i,j}(\mathbf{r}, \mathbf{r}') = \\ = \sum_{j=1}^M \frac{\partial \varphi_j(\mathbf{r}')}{\partial n} B_{i,j}(\mathbf{r}, \mathbf{r}') \end{aligned} \quad (42)$$

To form a set of linear algebraic equations, we take each node in turn as a load point  $\mathbf{r}$  and perform the integrations indicated in Eq. (42). This will result in the following matrices:

$$[\mathbf{A}][\boldsymbol{\varphi}] = [\mathbf{B}] \left[ \frac{\partial \boldsymbol{\varphi}}{\partial n} \right], \quad (43)$$

where the matrices  $[\mathbf{A}]$  and  $[\mathbf{B}]$  contain the integrals of the kernel's normal derivative  $\frac{\partial G(|\mathbf{r} - \mathbf{r}'|)}{\partial n}$  and the kernels  $G(|\mathbf{r} - \mathbf{r}'|)$  respectively, i.e., the functions  $A_{i,j}$  and  $B_{i,j}$  of Eq. (42).

Therefore, the kernel derivative with respect the normal direction in the collocation point can be expressed:

$$\frac{\partial G(|\mathbf{r} - \mathbf{r}'|)}{\partial n} = -\frac{i}{4} k H_1^{(1)}(k|\mathbf{r} - \mathbf{r}'|) \left( \frac{x-x'}{r} n_x + \frac{y-y'}{r} n_y \right) \quad (44)$$

where  $H_1^{(1)}$  is the spherical Hankel function of the first kind and of order one.

The integrand after the subtracting out procedure is regular with the separated singular term which could be calculated analytically (see for example [1, 3]).

Inside the domain which is the interior of a square (like the one presented in Fig. 1) but of side equal to 1 m and origin of cartesian system is in the left lower corner. Then distribution of the velocity potential  $\varphi$  as analytical solution is equal to:

$$\varphi(\mathbf{p}) = \sin\left(\frac{k}{\sqrt{2}}x\right) \sin\left(\frac{k}{\sqrt{2}}y\right) \quad (45)$$

This equation (45) is the solution of the Helmholtz equation (see Eq. (40)) with the following boundary condition. On the part of the boundary the Dirichlet boundary conditions are imposed:

$$\varphi(\mathbf{p}) = \begin{cases} 0 & \text{on } \Gamma_2 \text{ when } x = 0 \\ 0 & \text{on } \Gamma_3 \text{ when } y = 0 \end{cases} \quad (46)$$

and on the other part:

$$\varphi(\mathbf{p}) = \begin{cases} \sin\left(\frac{k}{\sqrt{2}}a\right) \sin\left(\frac{k}{\sqrt{2}}y\right) & \text{on } \Gamma_4 \text{ when } x = 1 \\ \sin\left(\frac{k}{\sqrt{2}}x\right) \sin\left(\frac{k}{\sqrt{2}}a\right) & \text{on } \Gamma_1 \text{ when } y = 1 \end{cases} \quad (47)$$

where  $a = 1\text{m}$  is the size of the square region.

For above Dirichlet boundary conditions solution and the equipotential lines are presented in the below figures:

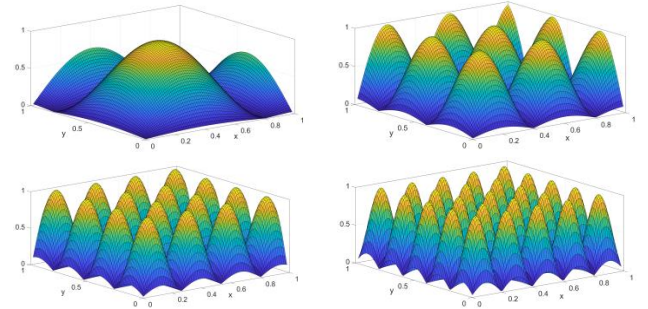


Fig. 7. Potential surface over the region of interest for different frequency of excitation

Drawing of equipotential lines corresponding to the velocity potential surface (above) for different frequencies with marked points for which the mean relative error was calculated (see table 1 and 2) and the equipotential lines are presented below (Fig. 8). The choice of these checkpoints is a compromise between points that define equipotential lines (too many) and a small number of points that could reliably reflect the mean relative error of the calculations. Their location is shown in the Fig. 8.

As the analytical solution is known (see Eq. 45) then the measure of error could be calculated only in special points shown in Fig. 8.

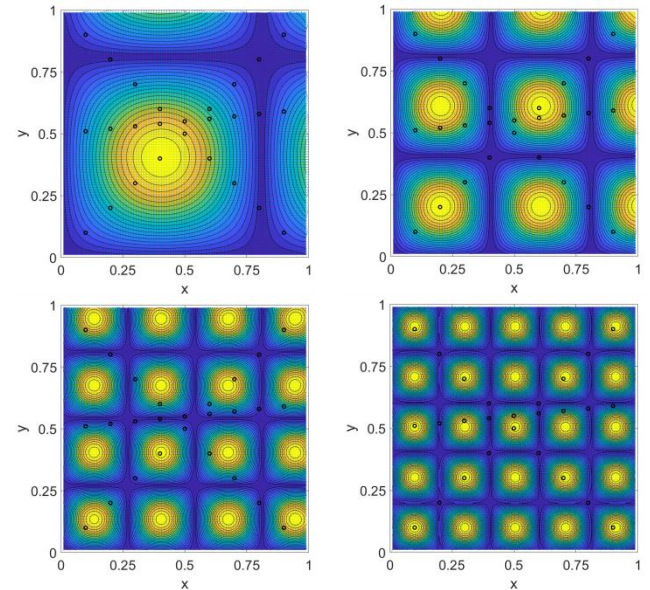


Fig. 8. Region of interest and equipotential lines distribution for different frequency excitation

The points are selected in such a way as to provide a comparison of the analytical solution with the numerical one for the entire range from minimum to maximum absolute values of the velocity potential. Therefore, the above method can be taken as an estimation of the accuracy of the calculations.

The measure of error used to estimate the accuracy of the subtracting out method is the mean relative error (MRE):

$$MRE = \frac{1}{N} \sum_{j=1}^N \frac{|\widehat{\varphi}_j - \varphi_j|}{|\varphi_j|} \quad (48)$$

where  $\widehat{\varphi}_j$  and  $\varphi_j$  are the numerically computed and analytical values of  $\varphi$  at the specially selected points presented in Fig. 8.

The basic acoustic data for benchmark calculation are presented in table 1. In Fig. 9 there is a graphical representation of the mean relative error versus frequency when the discretization of the area remains constant. It is well known that the number of boundary element per wavelength must be between 10 to 8 or 6. The lower limit strongly depend on the problem.

Table 1. Basic data for acoustic benchmark calculation

f [Hz]	300	600	900	1200
MRE [%]	0.66	5.35	6.97	32.55
k [1/m]	5.47	10.96	16.44	21.92
λ [m]	1.15	0.57	0.38	0.29
element length [m]	0.0833	0.0833	0.0833	0.0833
max arg. of Henkel function	0.1966	0.3932	0.5898	1.977
no of BE per λ	13.8	6.8	4.6	3.5

As we can see the subtract out procedure of singular integrals calculations provide reliable results. If all standards of acoustic calculations are preserved than the mean relative error is extremely low (see the first column of the table 1).

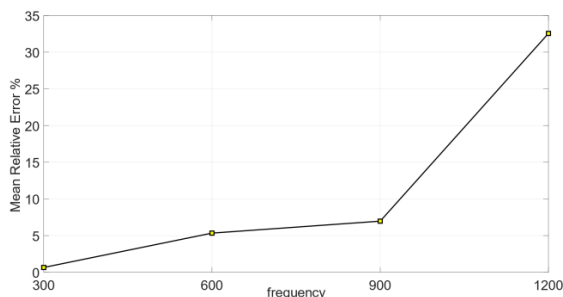


Fig. 9. Mean Relative Error versus frequency for constant discretization

To check the influence of subtracting out procedure on the calculations, the number of the elements per wavelength was kept constant on the level of a little bit more seven. Then the mean relative error for different frequency oscillated between 1 and 4.7% (see the table 2). It is worth to notice that for the highest frequency equal to 1200 Hz the error is only 1.15%.

Table 2. Basic data for acoustic benchmark calculation

f [Hz]	300	600	900	1200
MRE [%]	2.00	4.72	0.97	1.15
k [1/m]	5.48	10.96	16.44	21.92
λ [m]	1.15	0.57	0.38	0.29
element length [m]	0.1667	0.0833	0.0556	0.0417
max arg. of Henkel function	0.45	0.45	0.393	0.393
no of BE per λ	6.88	6.88	6.88	6.88

The results are quite satisfactory, and the maximal error is less than 5%.

## 6. Conclusions

In this paper the methods of logarithmic singularity in 2D space were considered.

Of the many different methods, only two have been considered, namely the method of ignoring singularities and the method of subtracting out singularity. The first method is presented on the example of a boundary element of the second order. As a result of the numerical experiment, this method was assessed as ineffective.

The second method is similarly presented on the example of a three-node boundary element of the second order for the Laplace equation. This case is a bit more complicated, because in one element in each of the three nodes we have singularities. It shows how a singular part can be extracted from an integrand function. The procedure is tedious and such a separation is not always possible due to the arithmetic intricacies.

Therefore, another way was indicated, illustrating it with an acoustic example. The kernels for acoustic problem are so complicated that, to simplify this problem, it was decided to use a constant element where the singularity occurs only in one node. The numerical experiment confirmed the efficiency and accuracy of this method.

## References

- [1] Aliabadi M. H.: The Boundary Element Method, Volume 2, Applications in Solids and Structures. John Wiley & Sons, LTD, 2002.
- [2] Harwood A. R. G.: Numerical Evaluation of Acoustic Green's Functions. PhD School of Mechanical, Aerospace & Civil Engineering, University of Manchester, 2014.
- [3] Kirkup S.: The Boundary Element Method in Acoustics: A Survey. Appl. Sci. 9, 2019, 1642 [https://doi.org/10.3390/app9081642].
- [4] Rymarczyk T.: Tomographic Imaging in Environmental, Industrial and Medical Applications. Innovatio Press Publishing Hause 2019.
- [5] Sikora J.: Boundary Element Method for Impedance and Optical Tomography. Warsaw University of Technology Publishing Hause, Warsaw 2007.
- [6] Smith R. N. L.: Direct Gauss quadrature formulae for logarithmic singularities on isoparametric elements. Engineering Analysis with Boundary Elements 24, 2000, 161–167.
- [7] [https://www.comsol.com/acoustics-module] (available: 10.01.2024).
- [8] [https://reference.wolfram.com/language/PDEModels/tutorial/Acoustics/AcousticsFrequencyDomain.html] (available: 10.01.2024).
- [9] Gaussian Quadrature Weights and Abscissae [po-max.github.io] (available: 10.01.2024).

Prof. Tomasz Rymarczyk  
e-mail: tomasz@rymarczyk.com

He is the director in Research and Development Centre in Netrix S.A. and the director of the Institute of Computer Science and Innovative Technologies in the University of Economics and Innovation, Lublin, Poland. He worked in many companies and institutes developing innovative projects and managing teams of employees. His research area focuses on the application of non-invasive imaging techniques, electrical tomography, image reconstruction, numerical modelling, image processing and analysis, process tomography, software engineering, knowledge engineering, artificial intelligence, and computer measurement systems.



Prof. Jan Sikora  
e-mail: sik59@wp.pl

Prof. Jan Sikora (Ph.D. D.Sc. Eng.) graduated from Warsaw University of Technology Faculty of Electrical Engineering. During 50 years of professional work, he has obtained all grades, including the position of full professor at his alma mater. Since 1998 he has also worked for the Institute of Electrical Engineering in Warsaw. In 2008, he has joined Electrical Engineering and Computer Science Faculty in Lublin University of Technology. During 2001–2004 he has worked as a Senior Research Fellow at University College London in the prof. S. Arridge's Group of Optical Tomography.

